Available online at www.sciencedirect.com
ScienceDirect
Cement and Concrete Research 36 (2006) 1575 – 1582
Cement and Concrete Research

# Characterization of the water flow through concrete based on parameter estimation from infiltration tests

Vicente Navarro [a,*], Ángel Yustres [a], Luís Cea [b], Miguel Candel [a], Ricardo Juncosa [b], Jordi Delgado [b]

[a] Civil Engineering School, University of Castilla-La Mancha, Ciudad Real, Edificio Politécnico, 13071, Spain
[b] Civil Engineering School, University of A Coruña, A Coruña, Campus de Elviña, 15071, Spain

Received 18 October 2005; accepted 14 November 2005

**Abstract**

When considering the durability and performance of concrete structures, the characterisation of the moisture distribution becomes a question of major concern. In this paper, a new approach for the characterization of the flow parameters, either under saturated or partially saturated conditions, is presented. The method is based on numerical back-analysis of simple and inexpensive infiltration tests. The satisfactory results that were obtained support the validity of the methodology developed and point towards a promising new line of research. Further examples covering a wider casuistic of concrete types must be performed before the applicability of the method can become fully consolidated.


*Keywords:* Durability; Permeability; Transport properties; Moisture transfer

## 1. Introduction

It is generally agreed that the overall performance of concrete structures cannot be simply described by the quality of concrete in terms of its short-term resistant properties. Concrete durability is an important attribute when assessing long-term performance.

Concrete durability is not a simple property because it depends on many interrelated physical and chemical characters and processes (cement type, water/cement ratio, type and quality of aggregates, admixtures, manufacturing, loads, weather conditions, etc.). A key aspect of concrete durability stands on its flow properties. As pointed out in CEB/FIP Model Code 1990 [1], the durability of concrete structures against external aggressive chemical reactions depends, primarily, on the permeability of their surface layers, and although a huge experimental effort has been developed, we do not yet have any generally accepted method for the fast, economic, and accurate determination of the hydrodynamic properties of concrete. While such methods are not developed, concrete classification and/or prescriptions based on its performance against potentially aggressive environments will be a challenging task. This paper aims to offer a new approach for the determination of some of the water flow properties of concrete through the combination of a simple and inexpensive laboratory procedure, coupled to numerical analysis based on identification techniques implemented in an easy-to-use computer code.

## 2. Laboratory characterization of concrete permeability

The determination of concrete permeability has been experimentally analysed by different authors and several methods can be found within the concrete literature accounting for this topic. Perhaps, the simplest method is that which places a head of water above a concrete sample while monitoring over time the change of height of the water column to obtain the corresponding flow [2]. However, due to the low permeability of concrete, this method may take weeks or even longer before sufficient flow has been attained to accurately determine permeability [3]. To shorten the testing time, a common variation of this method (see, for instance, Refs. [4–6]) proposes the pressurization of water against one of the faces of the concrete test sample while ensuring an effective sealing to prevent water leakage through the sides of the sample. However, in the case of low-permeability concrete, if we want

* Corresponding author. E.T.S.I. Caminos, Canales y Puertos, Edificio Politécnico, Avda. Camilo José Cela s/n, 13071, Ciudad Real, Spain. Tel.: +34 926 29 53 00x3264; fax: +34 926 29 53 91.
*E-mail address:* Vicente.Navarro@uclm.es (V. Navarro).

0008-8846/$ - see front matter © 2005 Elsevier Ltd. All rights reserved.
doi:10.1016/j.cemconres.2005.11.015

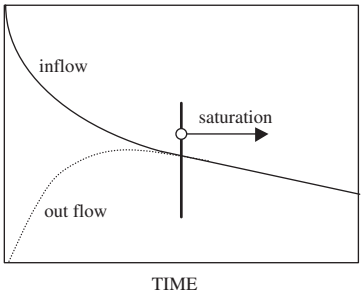


Fig. 1. Inflow and outflow rates for unsaturated concrete. When both curves coincide, saturation of concrete is usually assumed (adapted from [24]).

to be able to obtain accurate and reproducible permeability measurements, it is necessary to attain rather high water pressures [7]. In such situations, [3] has pointed the promising potential of triaxial-cell like techniques (see also [8]). A cylindrical specimen is housed into a pressurized sleeve to prevent any leakage through the sides. Then, a high-pressure gradient may be maintained across the sample to obtain adequate permeability measurements.

The methods described so far apply to water-saturated porous materials that contain virtually no air. However, it is difficult to achieve a saturated condition with many low-permeability concretes. With these materials, permeability is usually evaluated using the so-called penetration method ([9–11]). This method consists of the exposition of the top surface of cylindrical concrete samples to a given water pressure during 3–4 days. Then, the samples are cracked open (typically by means of a Brazilian test), and the average depth of water penetration is measured. It is worth mentioning that the permeability coefficient derived from this method is highly dependent on the time of the test. This dependence is commonly observed in unsaturated tests, where though the infiltration flux decreases as a function of time (Fig. 1), the corresponding permeability increases due to the progressive growth of the saturated area available to liquid water flow. The high initial water uptake must be understood as the response of the system to the high hydraulic gradients generated by the unsaturated concrete. Because the water located within the porous structure of "dry" concrete forms high curvature menisci—where, according to the Young–Laplace's equation (see Fig. 2), water is at much lower pressure than atmospheric—a high hydraulic gradient develops when one of the faces of the test specimen is exposed to pressured water. This hydraulic gradient is high enough to justify the initially high

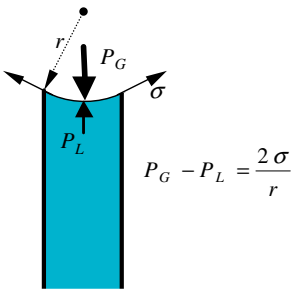


Fig. 2. Young–Laplace's equation. $\sigma$ represents the surface tension.

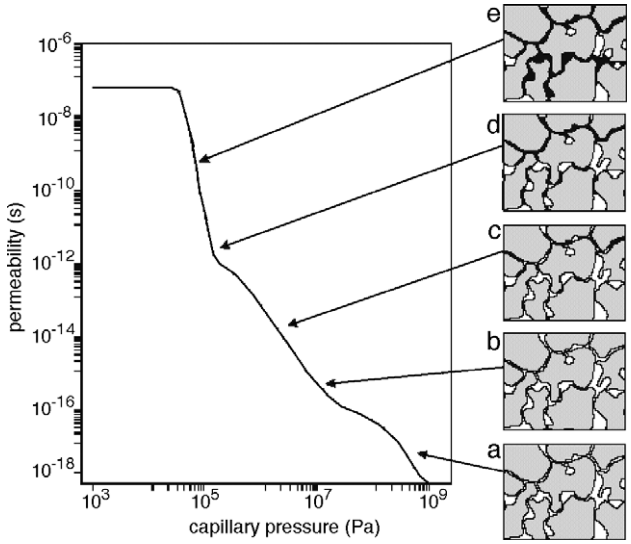


Fig. 3. Moisture permeability as a function of capillary pressure, and the corresponding filling of the pore space for a fictitious porous material. On the right, grey areas represent the material's matrix, while white areas represent pores filled with air, and black zones correspond to pores filled with liquid water. Once a continuous liquid phase is formed, the moisture permeability increases significantly. From [12].

water uptake in spite of the low permeability of dry concrete. However, as far as concrete becomes saturated, although permeability increases (Fig. 3), the water uptake curve progressively drops due to the progressive lowering of the hydraulic gradient. The process is further complicated by the fact that the moisture distribution within the sample at any time is not uniform, and because at any point of the sample the water content changes over time.

The accurate characterization of the complex flow process in concrete requires the adoption of a sound conceptual model which must be able to account for the water flow through partially or fully saturated concrete materials. Such a conceptual model will not only improve the interpretation of permeability tests, but it will also make possible to describe the distribution of water content throughout entire concrete structures exposed to different environmental and/or manufacturing conditions. This is of paramount importance if we remember that deleterious processes like cement carbonation, chloride penetration and the concomitant loss of passivity and corrosion of steel reinforcement depend on the degree of concrete's saturation.

## 3. Conceptual flow model

Under service conditions, concrete saturation is low enough to ensure that each build-up in gas pressure will rapidly disappear, so that gas pressure remains at a constant atmospheric pressure [12]. Therefore, gas flux can be safely ignored [13]. Moreover, in our isothermal-infiltration tests, vapour flow plays a minor role. So, the flow problem will be simplified to the analysis of liquid water movement.

Liquid water flowing through porous media is usually modelled using a generalization of Darcy's Law. However, as we mentioned before, concrete permeability is not only

Table 1
Mix proportions and other physical properties of the used concretes

| Mix | $w/c$ | $M_W$ (kg/m$^3$) | $M_C$ (kg/m$^3$) | $M_S$ (kg/m$^3$) | $M_A$ (kg/m$^3$) | $\rho$ (kN/m$^3$) | $f_{ck}$ (MPa) | $\phi$ |
|---|---|---|---|---|---|---|---|---|
| NC | 0.4 | 184 | 450 | 505 | 657 | 24.3 | 55 | 0.11 |
| LC | 0.4 | 200 | 500 | 376 | 74 | 18.5 | 51 | 0.14 |

The expression $w/c$ is the water–cement ratio; $M_W$, $M_C$, $M_S$, and $M_C$ are, respectively, the masses of water, cement, sand and aggregate per volume unity of concrete; $\rho$ is the bulk density; $f_{ck}$ is the compressive strength at 28 days; and finally, $\phi$ is the porosity accessible to water.

dependent on the size and distribution of voids, but it also depends on the degree of saturation. Therefore, the permeability function is usually split into two distinct parts. The first one, $K$, which has area units, is called "intrinsic permeability" and strictly depends on the geometric properties of the porous media. When the porous media is saturated, $K$ is equal to the saturated permeability. The second function, $\kappa$, which is dimensionless, is known as "relative permeability" and depends on the degree of saturation (between 0 and 1) of the porous media. Taking these definitions into account, the volumetric liquid water flux (that is, the volume of liquid water that crosses a unit surface per unit time), $q$, can be computed as follows (Eq. (1)):

$$q = -\frac{K\kappa}{\mu_W}(\nabla P_L - \rho_W g k) \tag{1}$$

where $P_L$, $\mu_W$ and $\rho_W$ represent pressure, dynamic viscosity and density of liquid water, respectively. In turn, $g$ is the gravitational acceleration while $k$ is the unit vector pointing downwards in the direction of the gravity.

It is a well-known fact that, when relative permeability is defined as a function of suction (which, disregarding osmotic effects, can be defined as $s = P_G - P_L$, where $P_G$ represents the gas pressure), there is an important hysteresis, which nearly disappears if $\kappa$ is expressed in terms of the degree of saturation, Sr (defined as the quotient between the volumes of water and voids). Although there are several analytical models to account for hysteresis cycles (see [14], for instance), it is usual to simplify the flow model by using expressions of the relative permeability without taking into account any hysteresis. Some authors, Savage and Janssen among them [15], have proposed the use of the van Genuchten [16] formulation for concrete (Eq. (2)):

$$\kappa = \mathrm{Se}^{1/2}\left(1 - \left(1 - \mathrm{Se}^{1/m}\right)^m\right)^2 \tag{2}$$

where the relative degree of saturation, Se, is defined as $\mathrm{Se} = (\mathrm{Sr} - \mathrm{Sr_m})/(\mathrm{Sr} - \mathrm{Sr_M})$, being $\mathrm{Sr_m}$ the residual liquid saturation and $\mathrm{Sr_M}$ the maximum liquid saturation. Both $m$ and $\alpha$ are fitting parameters. Whereas $m$ is related to pore size distribution, $\alpha$ is related to air entry pressure. Parameter $m$ is also involved in the van Genuchten [16] water retention relationship (Eq. (3)):

$$\mathrm{Se} = (1 + (\alpha \cdot s)^n)^{-m} \tag{3}$$

where $n$, as $m$, is a fitting parameter related to pore size distribution. As usual, we have assumed that $m = 1 - 1/n$. Although there is also an important hysteretic effect in the relationship between Se and s [17], we have adopted the one-to-one relationship of Eq. (3). This simplification appears to be reasonable taking into account that some authors ([18,19]) indicate that, for most building materials, hysteretic phenomena is small enough to adopt as retention curve the main wetting path (absorption of an initially dry sample at hygroscopic humidity). On the other hand, [20] observed that, in the case of building materials showing a more pronounced hysteretic behaviour, their hygrothermal performance can be modelled satisfactorily by choosing a mean curve located at the midpoint between the drying and wetting curves.

For a given initial moisture distribution into a concrete element, the time evolution of water content in a concrete element can be computed upon resolution for a given boundary condition of the mass balance equation Eq. (4):

$$\frac{\partial(\rho_W \phi \mathrm{Sr})}{\partial t} + \nabla \cdot (\rho_W q) = 0 \tag{4}$$

where $\phi$ is the porosity accessible to water. Although in our model we are implicitly assuming isothermal conditions, and we are not taking into account any gaseous flux, the complexity of the problem requires the use of numerical techniques. Therefore, we have developed a finite element code which is able to simulate at a low computational cost the infiltration experiments described below.

## 4. Test procedure and results

Two different mixes were used, namely, normal-weight concrete ("NC") and structural lightweight concrete ("LC"). Portland cement CEM I-52.5 R [21,22] was used for both mixes. Normal-weight concrete was made with natural gravel, whilst the structural lightweight concrete was made with expanded shale as the coarse aggregate. River sand was the fine aggregate of both concretes. Mix proportions and other physical properties are given in Table 1. For both concretes the nominal maximum aggregate size was 10 mm. Therefore, provided that cylindrical samples of 100 mm diameter and 100 mm long were used, both the dimensional requirements prescribed by [8] (3 to 1) were accomplished.

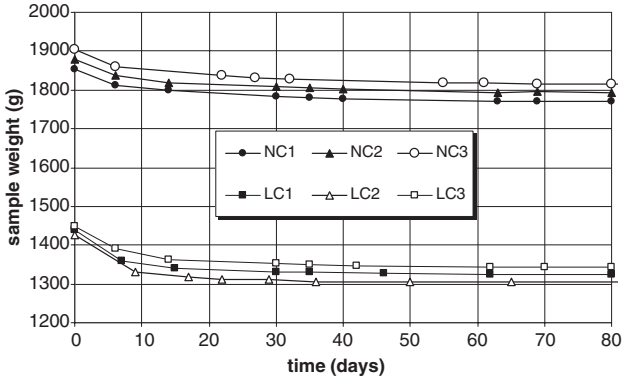


Fig. 4. Sample weight evolution when dried at 50 °C in a conventional oven prior to carry out the infiltration tests.

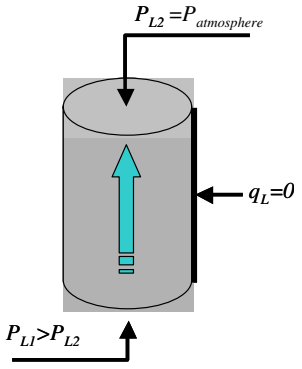


Fig. 5. Infiltration test schematic representation. Water is forced to enter through the base of a concrete specimen while zero lateral water flux boundary is granted using an impervious membrane. The upper surface is kept exposed to atmosphere in order to avoid the development of significant gas pressures that could make water uptake difficult.

Six specimens (three of NC and three of LC) were cured in a water bath for a continuous period of 8 months. Afterwards, to ensure low and uniform moisture contents, they were dried in an oven at 50 °C for about 80 days, under a constant mass (Fig. 4). The mean values of relative humidity and temperature during the drying was 78% and 11.9 °C. Accordingly, the initial suction of the specimens at the beginning of the experiments was about 320 MPa. Because this is an estimated value, we carried out a sensitivity analysis of the results based on the uncertainty in the initial suction. This analysis indicates that a change of ±20 MPa in the initial suction value translates in changes in the estimated parameters of less than 0.1%.

A triaxial cell [7,8] was used to perform the infiltration tests. The lower face of the test sample was subjected to an applied pressure of 500 kPa while the opposite face (top face) was kept open to atmospheric pressure (see Fig. 5). The top face was covered with a dry porous stone of very low air entry value (that is, high pore size), which allowed the air to outflow the sample while avoiding the build-up of any gas pressure when the saturation front advanced. In addition, to hinder any type of lateral water outflow, the concrete cylinders were surrounded by pressurized impervious membranes.

For the isothermal tests carried out, if porosity is assumed nearly constant, and neglecting the effect of chemical reactions,

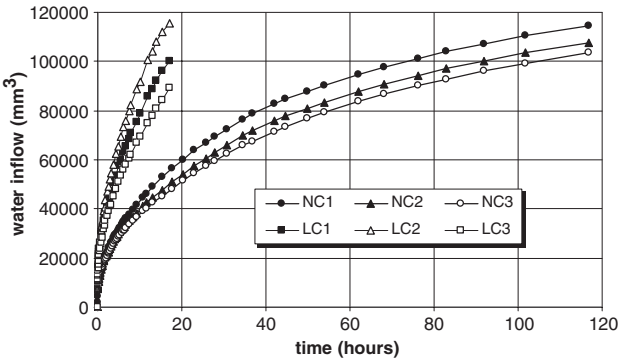


Fig. 6. Infiltration tests results: recorded water inflow as a function of time for each of the samples studied.

Table 2
Amount of water when starting the drying in the oven, $M1$, at the end of the drying (constant mass), $M2$, and at the end of the infiltration test, $M3$

| Sample | $V$ ($cm^3$) | $M1$ (g) | $M2$ (g) | $M3$ (g) | $\phi_1=(M1-M2)/V$ | $\phi_1=(M3-M2)/V$ |
|---|---|---|---|---|---|---|
| NC1 | 754.0 | 1854 | 1771 | 1854 | 0.110 | 0.100 |
| NC2 | 769.7 | 1880 | 1793 | 1876 | 0.113 | 0.108 |
| NC3 | 785.4 | 1903 | 1814 | 1893 | 0.113 | 0.113 |
| LC1 | 785.4 | 1439 | 1323 | 1425 | 0.148 | 0.130 |
| LC2 | 377.0 | 1427 | 1304 | 1420 | 0.156 | 0.147 |
| LC3 | 785.4 | 1450 | 1343 | 1435 | 0.139 | 0.120 |

$\phi_1$ and $\phi_2$ are accessible porosities associated with these water contents.

according to the flow model defined in Eqs. (1)–(4) the water inflow $Q_i$ entering through the base of the samples at any given time $t_i$ is a function of the parameters $K$, $Sr_m$, $Sr_M$, $\alpha$ and $m$, and identification techniques may be applied to obtain the value of the parameters which makes more probable that the data set $\{Q_i\}$ occurred.

Recorded water inflow is represented in Fig. 6. Complete saturation was achieved in about 37 h after the beginning of the experiments, for concrete NC, and 18 h for concrete LC. In that time, the amount of water that entered almost compensated the mass lost during drying in the oven (see Table 2). The accessible porosity seems to be properly characterized, and it is determined by averaging the values of Table 2 (means are shown in Table 1). Moreover, the residual liquid saturation, $Sr_m$, is taken as equal to 0, while the maximum liquid saturation, $Sr_M$, takes a value of 1. As a result, the parameter estimation process may become significantly simplified, provided that we only need to identify the three independent parameters $K$, $\alpha$ and $m$.

Once the experiments were completed, we conducted saturated permeability tests [23] whose results are presented in Table 3 and Fig. 7. The saturated permeabilities obtained let us validate the values of the intrinsic permeability identified from the infiltration tests.

Furthermore, in order to validate the parameters identified related with the retention curve, we conducted an additional battery of desiccation experiments. In these tests, carried out in a temperature-controlled room, the relative humidity was controlled by the vapour equilibrium technique (see Ref. [24], for instance). The tests are similar to those carried out by [15]. Five desiccators at 97%, 94%, 70%, 37% and 19%

Table 3
$K_S$, saturated permeabilities computed after the saturated permeability tests

| Sample | $K_S$ ($m^2$) $\times 10^{19}$ | $\alpha_D$ ($Pa^{-1}$) $\times 10^8$ | $m_D$ | $K_I$ ($m^2$) $\times 10^{19}$ | $\alpha_I$ ($Pa^{-1}$) $\times 10^8$ | $m_I$ |
|---|---|---|---|---|---|---|
| NC1 | 2.37 | 1.89 | 0.44 | 2.52 | 2.89 | 0.63 |
| NC2 | 3.01 | | | 2.71 | 2.53 | 0.55 |
| NC3 | 2.52 | | | 2.97 | 1.98 | 0.50 |
| LC1 | 9.01 | 2.67 | 0.40 | 9.31 | 2.7 | 0.54 |
| LC2 | 9.30 | | | 9.49 | 3.0 | 0.60 |
| LC3 | 8.83 | | | 9.23 | 2.5 | 0.50 |

$\alpha_D$ and $m_D$, fitting parameters of the desiccation tests (dotted lines in Fig. 9). These parameters where obtained from least-squares fitting of experimental points (dots in Fig. 9). $K_I$, $\alpha_I$, and $m_I$ are the identified parameters from the infiltration tests.

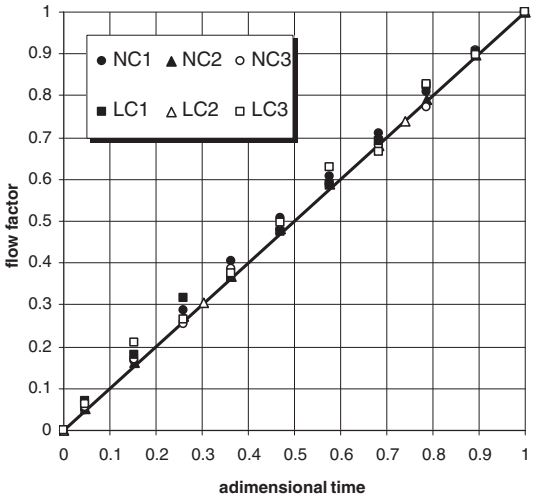


Fig. 7. Results of permeability tests performed after saturated conditions. The adimensional time is the ratio between current time and test duration (about 9.5 h). The flow factor is the ratio between the current accumulated water inflow and the total water inflow at the end of the test.

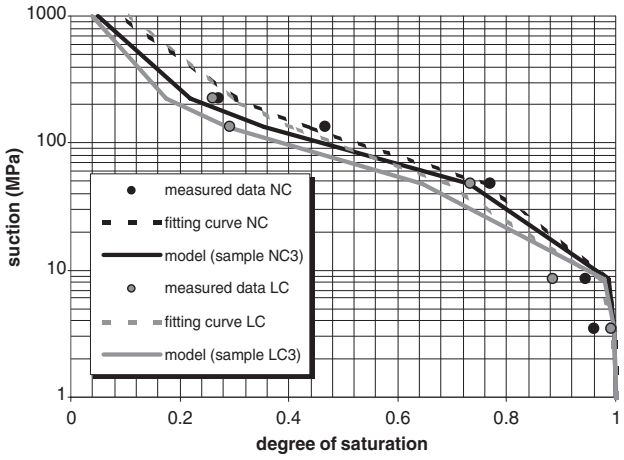


Fig. 9. Experimental retention curves obtained from individual tests conducted in the desiccators compared to the ones computed using the automatic parameter identification process. Dots are related with experimental results. Dotted lines are the fitting lines of these points when van Genuchten law Eq. (3) and least squares identification method are used. Continuous lines are obtained from the identification process carried out using the infiltration results. Black lines are related to the concrete NC and grey lines are related to the concrete LC.

were used. One 40-mm-thick saturated sample of concrete was placed into each one of them until reaching equilibrium. All specimens were weighed initially and at subsequent intervals throughout the drying process (see Fig. 8). From the water content at equilibrium, the retention curve of both concretes was deduced (Fig. 9). The fitting parameters of these curves are given in Table 3.

## 5. Parameter identification

To keep the method as simple and practical as possible, we decided to base the parameter identification only on the recorded water inflow monitored over time, $\{Q_i\}$. Therefore, the initial constrains for the parameter identification (i.e., the 3D space of all feasible parameters or "search space") will be large. It is a plausible situation that the selected objective function ("error") could eventually present local minima, and therefore, it is very important to characterize the topography of error.

Provided the accuracy of the flow measurement system (1 $mm^3$), the experimental data was directly used in the identification process without any treatment. Likewise, all experimental data is equally reliable, so we have selected a least squares fitting criteria. In order to describe the change of the root mean square error (rmse), we have developed a systematic sampling algorithm along the search space which generates a dense population of parameter vectors and computes, and afterwards, the error associated to each of them. Fig. 10 related to the first infiltration test of the sample NC1 (see Figs. 5–7), and represents an example of this procedure, adopting a constant $K$ equal to the identified optimum value ($K = 2.52 \times 10^{-19}$ $m^2$), and showing a cross section of the rmse

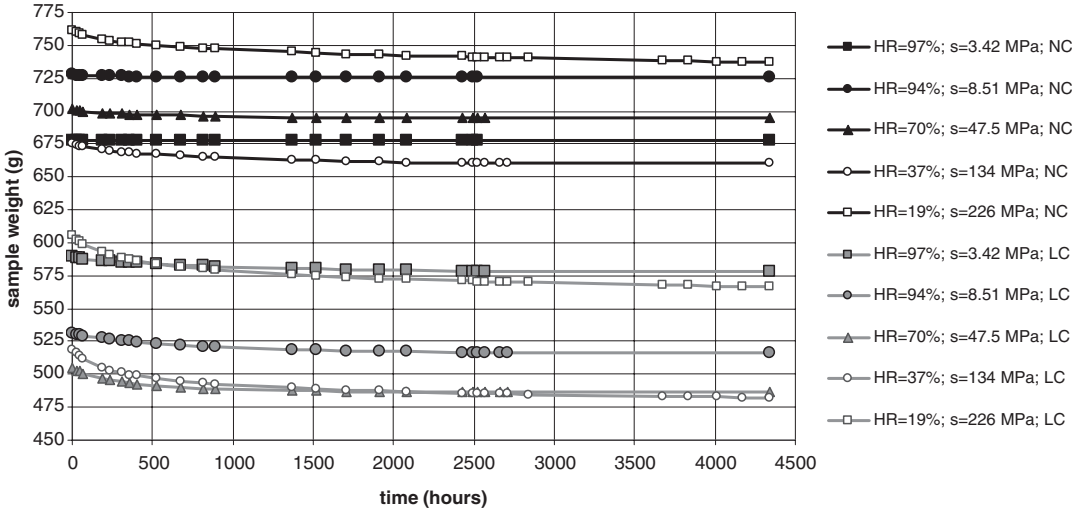


Fig. 8. Evolution of sample weight as a function of time measured in the desiccators. Relative humidity (HR) and associated suction (s) are indicated in the legend. Black lines are related to normal-weight concrete (NC) whilst grey ones are related to structural lightweight concrete (LC).

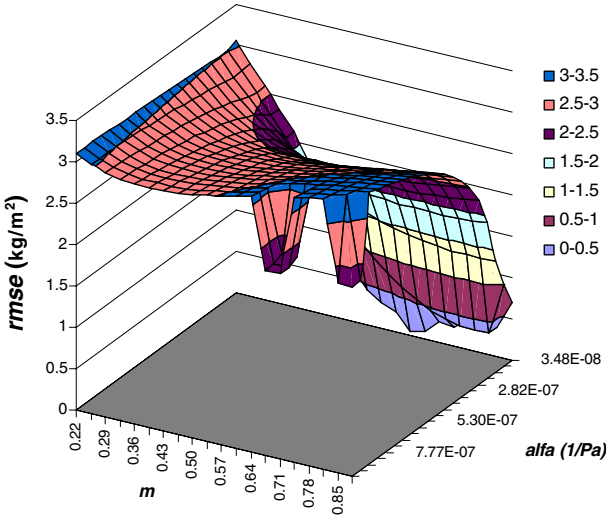


Fig. 10. Change in the square root of the mean quadratic error (rmse) computed for sample NC1. Permeability has been set equal to $2.52\times10^{-19}$ m$^2$ and a cross section of the rmse surface is done at the value of $\alpha$ where the rmse is minimum.

surface at its minimum. It can be seen that there are several local minima. If the identification were performed using gradient-based techniques (like Gauss–Newton or Levenberg–Marquardt) or other numerical techniques highly dependent on the initial estimates of the parameters (for instance, Powell's methods), there would have been a significant chance that the solution found was, in fact, a local minimum instead of the absolute one. Moreover, when using a Gauss–Newton-based algorithm and taking as initial values the parameters proposed by [15], the minimum found ($K=5.0\times10^{-19}$ m$^2$, $\alpha=1.0\times10^{-7}$ Pa$^{-1}$ and $m=0.5$) had a corresponding rmse of 0.15 while when using our systematic sampling algorithm we obtained an rmse of 0.04 (minimum $K=2.52\times10^{-19}$ m$^2$, $\alpha=2.89\times10^{-8}$ Pa$^{-1}$ and $m=0.63$). It is worth mentioning that, by applying the systematic sampling, histograms like that of Fig. 11 can be obtained to evaluate the confidence on the identified parameters.

The basic identification solver can be obtained upon request addressed to the first author.

## 6. Applicability of the method

From the point of view of the normal practice in civil engineering, once the experimental procedure and the numerical strategy needed to identify our selected flow parameters are defined, the value of the method is greatly conditioned by the time needed to perform the tests. In our experiments, full saturation of the concrete samples required a minimum of nearly 3 days, and an additional day is needed to make the test under saturated conditions. Thus, 4 days would be needed in order to determine $K$. Therefore, the proposed method takes almost the same time as the penetration method (see, for instance, [9]). However, although the duration of both kinds of experiments is comparable, the methodology that we propose in the present paper is able to characterize more flow parameters ($K$, $\alpha$ and $m$) than the single one ($K$) obtained with the alternative. Nonetheless, it would be interesting to reduce the duration of the experiments in order to retrieve accurate information as fast as possible. In that context, our numerical approach makes possible to make some estimations on the feasibility of such idea.

For the sample NC1, we have solved the identification problems based upon experimental data for six different test durations: (i) 3803 s (~1 h), (ii) 7869 s (~2 h), (iii) 22,138 s (~6 h), (iv) 41,632 s (~12 h), (v) 82,646 s (~3 h), and (vi) 132,956 s (~37 h). The last run corresponds with the time required to achieve full saturation of the test specimen. By reducing the duration of the test, we are able to test the predictive capability of our model to estimate the flow parameters. Such a scenario is particularly interesting in cases where rapid identification of parameters is important, where there is a large number of samples to be tested, or to take advantage of incomplete, otherwise useless, infiltration tests. It is worth noting that, although each one of the identification processes leads to a good fit (see Fig. 12), the parameters identified change in accordance with the length of the test. Nevertheless, as Fig. 13 shows, when we introduce more information to the process, let us say after the third run (that is, four times equal or higher than 6.15 h), the solution becomes stable, and the parameters are clearly identified. Such encouraging results seem to support the capability of this approach, although it is acknowledged that it is required a larger casuistic (different concrete types, specimen sizes, etc.) before concluding that parameter identification is a qualified technique able to predict flow parameters from extremely short infiltration experiments.

Table 3 displays the results of the identified parameters after modelling runs covering experimental times of 6.15 h or more. It can be seen that for both concretes, there is a significant

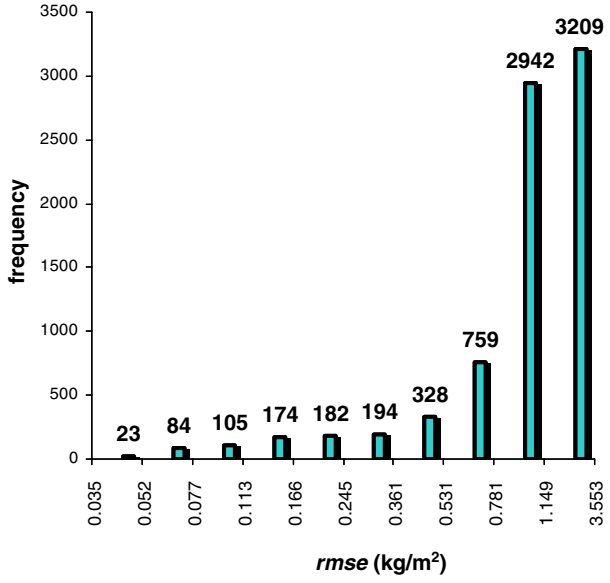


Fig. 11. Histogram showing the root mean square error, rmse, corresponding to specimen NC1. Only the 0.3 % of the identified parameters (23 over a total of 8000) define an rmse error less than the 1% of the maximum error recorded in the search space ($rmse_{MAX}=3.553$ kg/m$^2$ ). This observation provides a high confidence in the fact that these parameters are very close to the true absolute minimum.

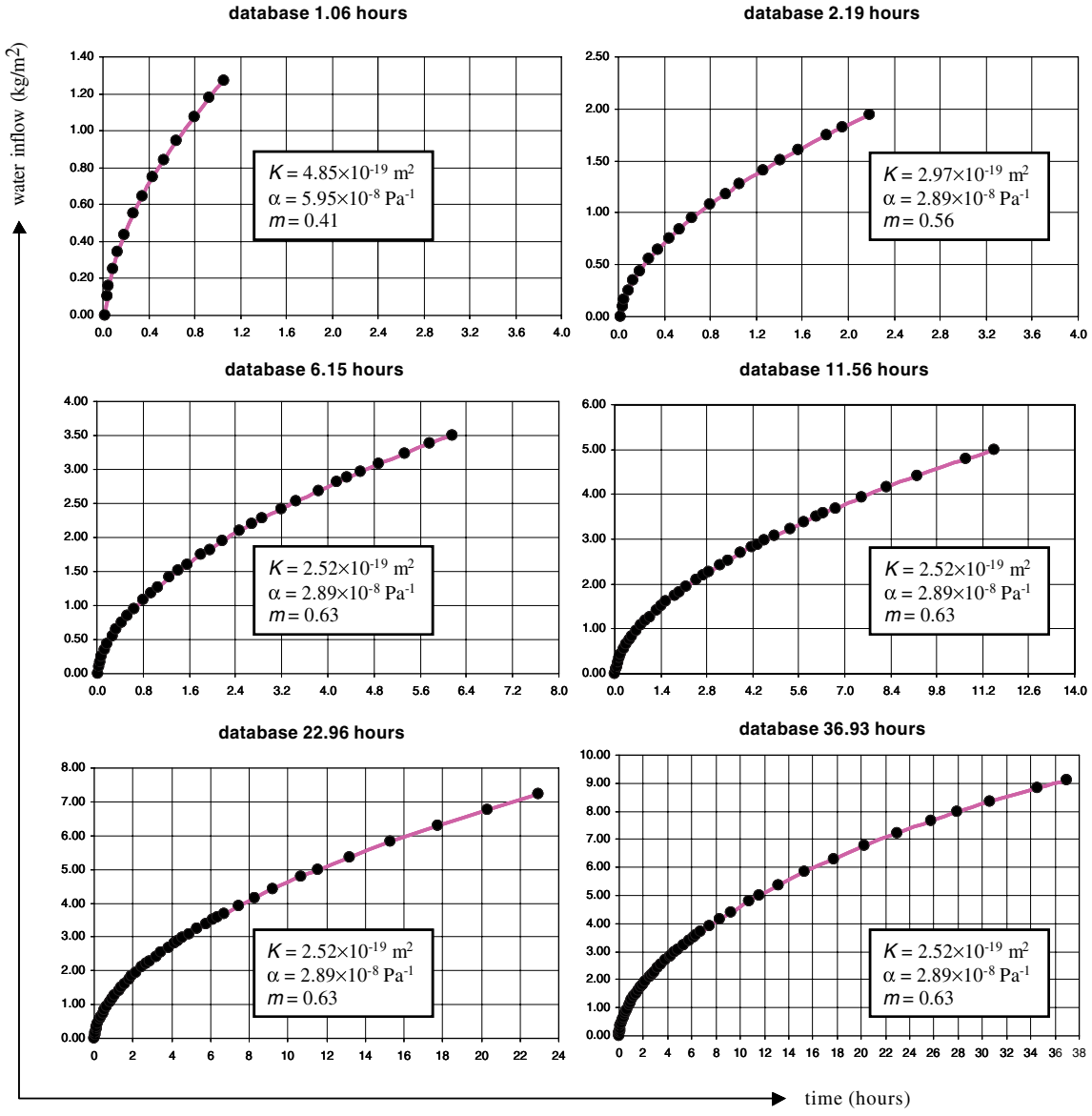


Fig. 12. Best-fit obtained in each one of the identification problems carried out using data from NC1. Experimental data, dots; model, continuous line.

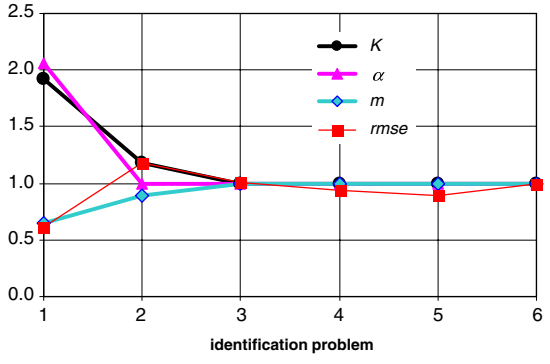


Fig. 13. Evolution of identified parameters ($K$, $\alpha$ and $m$) and of the square root of the mean error (rmse) for six different identification problems solved using data from sample NC1. Test durations are 1.06, 2.19, 6.15, 11.56, 22.96, 36.93 h, respectively. All the parameters shown and rmse are dimensionless with respect to their corresponding values for 36.93 h.

consistency in the results, and that there exists a good correlation in terms of saturated permeability. Good agreement is obtained when we compare the parameters $\alpha$ and $m$ of the retention curve identified by this method and by using the desiccators.

It should be stressed that we have used hardened concrete, and we will not include the uncertain effect of processes like the permanent self-sealing effect, autogenous sealing or the continuing hydration [25]. All these processes are related to changes in the permeability and/or porosity structure of concrete. Therefore, there is a chance for young or cracked concretes because these materials flow properties may change during the test, which would make the application of the proposed approach useless.

## 7. Conclusions

The approach presented in this paper contributes to the characterization of concrete's flow properties. It is based on

simple and inexpensive infiltration tests associated with a numerical identification of relevant flow parameters from recorded values of water uptake by tests specimens. Moreover, the method does not require lengthy laboratory procedures. Therefore, provided that the numerical approach is highly automated, the proposed approach accomplishes its aim of simplicity and feasibility. The satisfactory results obtained in the modelling process, furnish some indications about the ability of our approach to model the water flow through concrete materials, both under saturated or partially saturated conditions. This represents a significant advance with regard to other methods, which only are able to render information related with the saturated behaviour. In addition, the proposed methodology seems to be able to appreciably reduce the time needed for the experimental characterization of infiltration tests.

It must be stressed however, that our encouraging conclusions represent a preliminary approach and that, in order to prove its soundness, it is necessary to conduct a wider survey of experiments, covering different types of cement, aggregates and mixes.

## Acknowledgements

The authors acknowledge the support provided by the Spanish Ministry of Foment through a research grant furnished in 1999, within the framework of key-actions research in Civil Engineering, Transport and Communications. It is also gratefully appreciated the research grant provided by the University of Castilla-La Mancha during the years 2002 and 2003.

## References

[1] CEB-FIP Model Code 1990, Design Code, Comité Euro-International du Béton, Thomas Telford Services Limited, London, 1993.
[2] D. Ludirdja, R.L. Berger, J.F. Young, Simple method for measuring water permeability of concrete, ACI Mater. J. 86 (5) (1989) 433–439.
[3] N.S. Martys, Survey of Concrete Transport and their Measurement, Document NISTIR 5592, National Institute of Standards and Technology, U.S. Department of Commerce, Gaithersburg, 1995.
[4] Réunion Internationale des Laboratoires d'Essais et de recherche sur les Matériaux et les Constructions (RILEM), Test for permeability of porous concrete, Recommendation CPC 13.2, 1979.
[5] International Standards Organization (ISO), Concrete Hardened-Determination of Permeability, Standard ISO/DIS 7032, 1983.
[6] A. Bisaillon, V.M. Malhorta, Permeability of concrete under uniaxial water-flow method, in: D. Whiting, A. Walitt (Eds.), ACI SP-108 Permeability of Concrete, Farmington Hills, 1988, pp. 175–193.
[7] A.S. El-Dieb, R.D. Hooton, Water-permeability measurement of high performance concrete using a high-pressure triaxial cell, Cem. Concr. Res. 25 (6) (1995) 1199–1208.
[8] Corps of Engineers Standards, Test method for water permeability of concrete using triaxial cell CRD-C 163-92, Handbook for Concrete and Cement, See the web site http://www.wes.army.mil/SL/MTC/handbook/handbook.htm, 1992.
[9] European Standard EN 12390-8, Testing Hardened Concrete. Part 8: Depth of Penetration of Water Under Pressure, European Committee for Standardization, Bruxelles, 2001, 10 pp.
[10] Réunion Internationale des Laboratoires d'Essais et de recherche sur les Matériaux et les Constructions (RILEM), Test for the penetration of water under pressure on hardened concrete, Recommendation CPC 13.1, 1979.
[11] International Standards Organization (ISO), Concrete hardened. Determination of the depth of penetration of water under pressure, Standard ISO/DIS 7031, 1983.
[12] S. Roels, Modelling unsaturated moisture transport in heterogeneous limestone, Ph. D. Thesis, Catholic University of Leuven, Leuven, Belgium; 2000.
[13] F. Descamps, Continuum and discrete modelling of isothermal water and air transfer in porous media, Ph. D. Thesis, Catholic University of Leuven; Leuven, Belgium, 1997.
[14] Y. Mualem, Hysteretical models for prediction of the hydraulic conductivity of unsaturated porous media, Water Resour. Res. 12 (6) (1976) 1248–1254.
[15] B.M. Savage, D.J. Janssen, Janssen, Soil physics principles validated for use in predicting unsaturated moisture movement in portland cement concrete, ACI Mater. J. 94 (1) (1997) 63–70.
[16] M.T. Van Genuchten, A closed-form equation for predicting the hydraulic conductivity of unsaturated soils, Soil Sci. Soc. Am. J. 44 (1980) 892–898.
[17] Y. Mualem, A conceptual model of hysteresis, Water Resour. Res. 10 (3) (1974) 514–520.
[18] H.M. Künzel, Zusammenhang zwischen der feuchtigkeit von außenbauteilen in der praxis und sorptionseigenschaften der baustoffe, Bauphysik 3 (4) (1982) 101–107.
[19] M. Krus, K. Kieβl, Determination of the moisture storage characteristics of porous capillary active materials, Mater. Struct. 31 (1998) 522–529.
[20] C. Rode, Combined heat and moisture transfer in building constructions, Ph. D. Thesis, Thermal Insulation Laboratory, Technical University of Denmark, 1990.
[21] European Standard EN 197-1, Cement–Part 1: Composition, Specifications and Conformity Criteria for Common Cements, European Committee for Standardization, Bruxelles, 2000, 30 pp.
[22] European Standard EN 197-1, ERRATUM. Cement–Part 1: Composition, Specifications and Conformity Criteria for Common Cements, European Committee for Standardization, Bruxelles, 30 pp., 2002.
[23] American Society for Testing Materials, ASTM D 5084-00, Standard Test Method for Measurement of Hydraulic Conductivity of Saturated Porous Materials Using a Flexible Wall Permeameter, Annual Book of ASTM Standards, 2004, pp. 1024–1036.
[24] A.-M. Tang, Y.-J. Cui, Controlling suction by the vapour equilibrium technique at different temperatures and its application in determining the water retention properties of MX80 clay, Can. Geotech. J. 42 (1) (2005) 287–296.
[25] N. Hearn, Self-sealing, autogenous healing and continued hydration: what is the difference? Mater. Struct. 31 (212) (1998) 563–567.